Quiet time magnetotail plasma flow: Coordinated Polar ultraviolet images and Geotail observations

A. Ieda,[1,2] J.-H. Shue,[3] K. Liou,[3] S.-I. Ohtani,[3] C.-I. Meng,[3] D. H. Fairfield,[4] T. Mukai,[1] Y. Saito,[1] S. Machida,[5] T. Nagai,[6] and G. K. Parks[7]

[1]   A search for fast flows in the plasma sheet during quiet times was conducted in order to further test the previously found close association between fast flows and auroral brightenings. We first identified "quiet intervals" of at least 30-min duration in the Polar ultraviolet global images of auroras. During 16 months of Polar observations from January 1997 through April 1998, 41 quiet intervals were identified when Geotail was between 8 and 31 R_E down the tail and within 10 R_E of the midnight meridian. Fast flows were more rare during the quiet intervals than at other times. For 4 of the 41 intervals identified, Geotail detected flows faster than 300 km s^{-1} in the plasma sheet. All the four flows were earthward parallel flows accompanied by northward magnetic field beyond 20 R_E, and there were no perpendicular flows faster than 300 km s^{-1}. To understand the nature of the fast (but not perpendicular) flows during the quiet intervals, an earthward flow at 21 R_E down the tail was studied in detail. The plasma beta was higher than unity during the earthward flow, but the fastest ion velocity moments consisted of the two counterstreaming components flowing along the magnetic field, a characteristic known to define the plasma sheet boundary layer. Our results further support the close association between auroral brightenings and clear fast flows as seen in previous studies, because no perpendicular fast flows were found during quiet intervals. Since some perpendicular flows slower than 300 km s^{-1} were found beyond ~20 R_E down the tail, a velocity of ~300 km s^{-1} appears to statistically make a difference in the geoeffectiveness of perpendicular flows.   *INDEX TERMS:* 2744 Magnetospheric Physics: Magnetotail; 2764 Magnetospheric Physics: Plasma sheet; 2407 Ionosphere: Auroral ionosphere (2704); 2760 Magnetospheric Physics: Plasma convection; 2788 Magnetospheric Physics: Storms and substorms; *KEYWORDS:* fast flows, aurora, quiet time, plasma sheet, magnetotail

1.   Introduction

[2]   The near-Earth neutral line model of substorm has been more successful than many other models in explaining magnetotail characteristics beyond ~10−20 R_E at the times of substorms [e.g., *Baker et al.*, 1996]. However, the

association between reconnection and development of auroras is far from being firmly established, because reconnection signatures inside ~30 R_E like tailward moving plasmoids [*Ieda et al.*, 2001] or earthward fast flows [*Nakamura et al.*, 2001] are associated with small auroral brightenings as well as breakups.

[3]   The average magnetic field in the magnetotail has a weak northward component originating from the Earth's dipole magnetic field, however, tailward fast (>300 km s^{-1}) plasma flows in the tail tend to be accompanied by southward magnetic field [*Nishida et al.*, 1981; *Hayakawa et al.*, 1982]. These southward fields are believed to be evidence for reconnection in the tail. Theoretically, reconnection yields tailward flow with southward magnetic field and earthward flow with northward magnetic field. *Nagai et al.* [1998] statistically studied times near substorm onsets identified by ground magnetic field and found that the earthward flow with northward magnetic field is seen earthward of 20−30 R_E and the tailward flow with southward magnetic field is seen beyond this region. This result

[1]Institute of Space and Astronautical Science, Sagamihara, Kanagawa, Japan.

[2]Now at Solar-Terrestrial Environment Laboratory, Nagoya University, Toyokawa, Aichi, Japan.

[3]Applied Physics Laboratory, Johns Hopkins University, Laurel, Maryland, USA.

[4]Laboratory for Extraterrestrial Physics, NASA Goddard Space Flight Center, Greenbelt, Maryland, USA.

[5]Department of Geophysics, Kyoto University, Kyoto, Japan.

[6]Department of Earth and Planetary Sciences, Tokyo Institute of Technology, Tokyo, Japan.

[7]Space Sciences Laboratory, University of California, Berkeley, California, USA.

can be interpreted that reconnection is occurring somewhere between 20 and 30 R_E at the onsets.

[4] On the other hand, it has been reported that earthward fast flows can also occur during relatively quiet intervals as identified with ground magnetic field observations [*Sergeev et al.*, 1986; *Baumjohann et al.*, 1989; *Ohtani et al.*, 2002]. However, ground magnetic field observations often fail to detect spatially localized disturbance that global images can detect. Moreover, some of these fast flows were actually associated with weak geomagnetic disturbance, for example, lower than 100 nT. In other words, whereas fast flows during nonsubstorm intervals have been already reported, whether or not they occur without small auroral brightenings remains unknown.

[5] Associations between fast flows in the near-Earth tail and auroral brightenings were recently studied by first identifying fast flows and then studying global auroral images. *Fairfield et al.* [1999] studied some earthward fast flow events and found that they were accompanied by auroral brightenings. This result was further supported by an extended study by *Nakamura et al.* [2001]. *Ieda et al.* [2001] studied tailward moving plasmoids, whose north-then-south variations in the magnetic field are strong evidence for near-Earth reconnection. They found that at least 80% of tailward moving plasmoids were accompanied by auroral brightenings. The association between plasmoids and brightenings was ambiguous for the remaining 20%, since there had already been some auroral activities ongoing. Thus fast flows are inferred to be almost always associated with auroral brightenings, but it is sometimes difficult to determine whether or not a brightening is occurring when there are preexisting auroras.

[6] In this paper, we try to further test the association from another point of view: Fast flows are not expected during quiet intervals as defined from global auroral images, if there are always auroral brightenings for fast flows. The purpose of this study is to test the absence of fast flows during quiet intervals by first identifying quiet intervals in global images and then studying flows in the tail.

[7] The other purpose is to clarify the association between slow flows and auroral brightenings. Fast flows usually explicitly or implicitly refer to the plasma velocity faster than $300-400$ km s^{-1} and are often required to be perpendicular to the magnetic field for the significance in the magnetic flux transport [e.g., *Fairfield et al.*, 1999; *Paterson et al.*, 1998]. In previous studies of the association between fast flows and auroral brightenings, only "clear" fast flows were studied and they were found to be associated with brightenings. Such "clear" fast flows were plasmoids [*Ieda et al.*, 2001] or flow bursts with strong flux transfer rate [*Nakamura et al.*, 2001]. On the other hand, it is not clear how "less clear" fast flows like perpendicular flows slower than $\sim$300 km s^{-1} or parallel flows are associated with brightenings. In this study, we also study whether or not these less clear flows can occur during quiet intervals.

[8] The quiet intervals in this study are defined by excluding not only breakups in global images but also small brightenings or pseudobreakups and even fading auroras. It is generally impossible to identify "perfectly" quiet intervals, because very localized or weak disturbance is likely to be common even during quiet intervals. Moreover, there may be no "perfectly" quiet intervals at all. Thus the quiet intervals in this study may include even weaker, smaller, or shorter duration disturbance that is hard to recognize in global images.

2. Data Set

[9] This study is based on simultaneous observations by the Geotail and Polar spacecraft for 16 months from 1 January 1997 through 30 April 1998. (Geotail plasma data after April 30, 1998 are still under calibration.) During this period, Geotail orbited in the solar-ecliptic plane and had perigee of $\sim$10 R_E and apogee of $\sim$30 R_E.

[10] The low-energy particle (LEP) instrument on board Geotail makes three-dimensional plasma measurements [*Mukai et al.*, 1994]. In our statistical survey, we used 12-s (four-spin period) averages of velocity moments of ions from 32 eV q^{-1} to 39 keV q^{-1}. We calculated ion velocity moments with an assumption that all ion species are protons. We also used 12-s (statistical survey) and 3-s (case study) averages of the magnetic field data obtained by the magnetic field (MGF) experiment, which was described in detail by *Kokubun et al.* [1994].

[11] The Polar ultraviolet imager (UVI) provides global imaging of auroras [*Torr et al.*, 1995]. In automatically identifying quiet intervals, we used 36-s exposure time, Lyman-Birge-Hopfield-long (LBHL, $\sim$1700 Å) images, which were usually taken every 3 min. In a case study, we also examined the 18-s exposure LBHL images. The spatial resolution of the images is $\sim$40 km when Polar vertically observes the polar ionosphere from its apogee of 9 R_E. UVI images will be shown in the altitude adjusted corrected geomagnetic (AACGM) coordinates [*Baker and Wing*, 1989].

3. Statistical Survey
3.1. Identification of Quiet Intervals

[12] To identify quiet intervals, we first removed dayglow from the images for the March-September period but made no correction on the images in the winter seasons (October–February) when it was less necessary. More explanation for this procedure is given by *Shue et al.* [2001]. We then averaged the photon counts over each grid of 0.5° in the magnetic latitude (MLAT) and 0.25 hours in the magnetic local time (MLT) for the target area of $60°-75°$ MLAT and $21-03$ MLT. We labeled the images as quiet when there were no more than one grid point with photon counts above a threshold of 10 photons cm^{-2} s^{-1} $\sim$300 Rayleigh. In other words, we ignored potential brightenings smaller than the one grid size or weaker than 10 photons cm^{-2} s^{-1}. Twenty percent of images are identified as quiet when Geotail was in $-8 \geq X > -31$ R_E and in $|Y| < 10$ R_E of the tail including both the plasma sheet and the tail lobe. There are no accepted quantitative criteria of brightenings. We chose the threshold as low as 10 photons cm^{-2} s^{-1}, to exclude brightenings that appeared in case studies by *Ieda et al.* [2001] and *Nakamura et al.* [2001]. We realize some quiet intervals might have been excluded due to occasional isolated noise recorded as higher than 10 photons cm^{-2} s^{-1}. A typical background noise level of the images is 4 photons cm^{-2} s^{-1}. Thus the quiet intervals in this study may sometimes include very weak brightening-like signatures
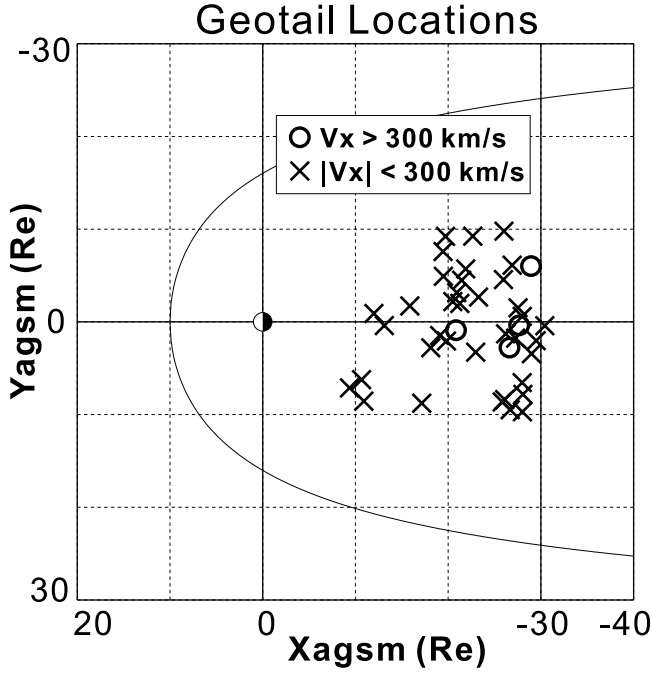
Figure 1. Geotail locations for 41 quiet intervals shown on the equatorial plane of the tail in the aberrated GSM coordinates. Circles indicate that Geotail observed flows faster than 300 km s^{-1} in the plasma sheet, and crosses indicate that Geotail observed no fast flows.

with 4–10 photons cm^{-2} s^{-1} that could be visually identified in fine spatial resolution images but are difficult to automatically discriminate from background noise or quiet time auroral ovals.

[13] Finally, we searched for intervals when all the 36-s exposure LBHL images remained quiet for at least 30 min with the time separation between images shorter than 4 min. As a result, we found 41 quiet intervals, totaling 39 hours, which was 8% of the 512 hours of Polar observations when the target area remained inside the field of view more than 30 min. The longest quiet interval continued for 126 min.

[14] Figure 1 shows the Geotail locations for the identified 41 quiet intervals, projected on the XY plane. We used the aberrated GSM coordinates with an aberration of 4°. Circles indicate that Geotail observed flows faster than 300 km s^{-1}, and crosses indicate the remaining intervals (without fast flows). Each circle or cross represents the Geotail location at the center time of each interval. Four intervals beyond 20 R_E included fast flows.

3.2. Occurrence of Flows

[15] Figure 2 shows the occurrence probabilities (%) of V_x, $V_{perp,x}$, and $V_{para,x}$ in the plasma sheet, from top to bottom. They are the X component of the plasma velocity and the X components of the velocity perpendicular and parallel to the magnetic field, respectively. The three panels on the left were obtained in $-8 \geq X > -20$ R_E, and the other three panels on the right were obtained in $-20 \geq X > -31$ R_E. Each panel shows the occurrence probabilities of the velocities in the plasma sheet for the quiet intervals (bold line), and all intervals including the periods without

the image data (thin line). The plasma sheet was identified by $\beta \geq 0.1$, where β is the ratio of the plasma pressure to the magnetic pressure. We used the measured ion temperature and assumed the ratio of ion to electron temperature as five [*Slavin et al.*, 1985]. The first and last 5 min of each quiet interval were excluded, because disturbance in the tail and associated auroras may be separated by a few minutes [*Ieda et al.*, 2001].

[16] The quiet intervals contain 2813 plasma sheet 12-s samples (equivalent to 9 hours) in $-8 \geq X > -20$ R_E and 4994 samples (17 hours) in $-20 \geq X > -31$ R_E, while the all-intervals data set contains 200,335 plasma sheet samples (668 hours) in $-8 \geq X > -20$ R_E and 266,808 samples (889 hours) in $-20 \geq X > -31$ R_E. Note that the occurrence probabilities below ~1% only contain less than a few tens of samples in the quiet intervals data set. Thus each occurrence probability of velocities faster than ~100 km s^{-1} during quiet times is not generalized but represents our specific data set. Occurrence probabilities of fast flows are also expected to depend on satellite locations, especially on the distance from the neutral sheet. Although we restricted our data set to the plasma sheet of limited XY locations, it is still possible that fast flows are more often found in more specific locations. However, it is currently difficult to take this effect into account and normalize the quiet time data set, because quiet time fast flows are quite rare.

[17] Fast flows ($|V_x| > 300$ km s^{-1}) during all intervals (thin lines) are more frequently observed in $-20 \geq X > -31$ R_E (top right panel of Figure 2) than in $-8 \geq X > -20$ R_E (top left panel of Figure 2), and this is consistent with the results of *Paterson et al.* [1998]. This is also in the case for the quiet intervals (bold lines). It appears in the top two panels of Figure 2 that fast flows ($|V_x| > 300$ km s^{-1}) are more rare during the quiet intervals (bold lines) when compared with the all intervals (thin lines), as is consistent with the results of *Baumjohann et al.* [1989]. However, a few earthward flows faster than 300 km s^{-1} were still found in the four intervals, whose Geotail locations are shown as circles in Figure 1. There were no tailward flows faster than 300 km s^{-1}, and the fastest tailward streaming plasmas ($V_x = -260$ km s^{-1}, $V_{perp,x} = -183$ km s^{-1}) were found in a fluctuating flow, but the magnetic field was northward (not shown).

[18] No perpendicular flows faster than 300 km s^{-1} were found during quiet intervals, as shown by the thin lines in the middle panels of Figure 2. There was a perpendicular flow faster than 200 km s^{-1} as shown by the thin line in the middle right panel of Figure 2 in a single interval but the magnetic field was almost steady (not shown). Thus it is not surprising that there was no auroral brightenings for the particular perpendicular flow, which recorded the maximal $V_{perp,x}$ (= 262 km s^{-1}) and the maximal flux transport rate ($V_x B_z = 2.6$ mV m^{-1}) during our quiet intervals. There were four intervals that contained perpendicular flows faster than 100 km s^{-1} but slower than 200 km s^{-1}, including transient events as shown later. These results indicate that perpendicular flows faster than 100 km s^{-1} but slower than 200–300 km s^{-1} are possible during quiet intervals.

4. Case Study

[19] Figure 2 suggests that quiet time flows were observed more frequently farther from the Earth. There were four
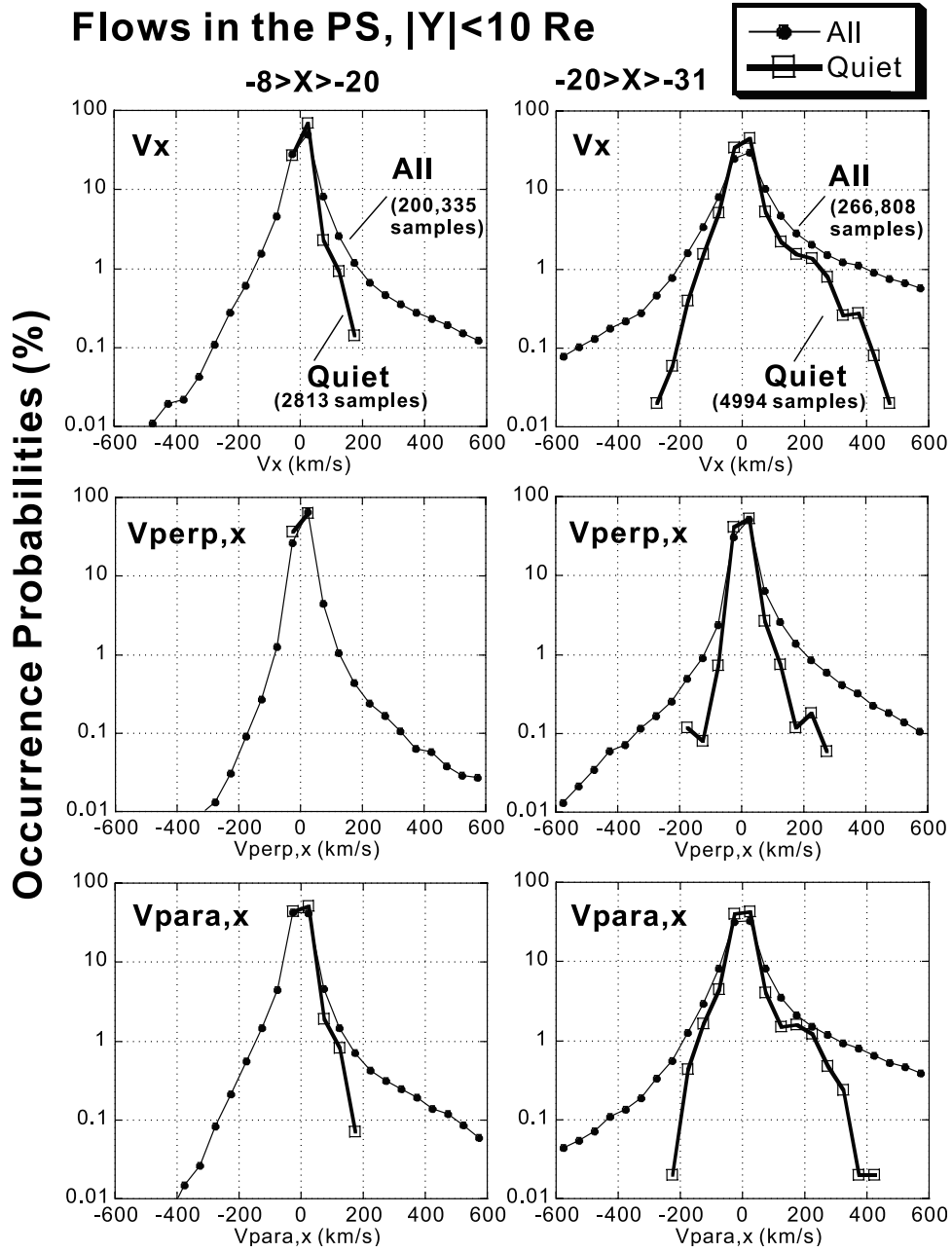
Figure 2. The occurrence probabilities (%) of (top to bottom) V_x, $V_{perp,x}$, and $V_{para,x}$ in the plasma sheet. The three panels on the left are obtained in $-8 \geq X > -20$ R_E, and other three panels on the right are obtained in $-20 \geq X > -31$ R_E. Each panel shows the occurrence probabilities for the quiet intervals (bold line) and for all intervals regardless of UVI observations (thin line). The plasma sheet was identified by $\beta \geq 0.1$.

intervals containing earthward fast flows in Figure 1. For the event closest to the Earth, Geotail observed an earthward flow at 21 R_E that occurred at 1346–1353 UT on 12 December 1997. This event was studied in detail.

[20] Figure 3 shows a 40-min series of Polar spacecraft UVI/LBHL fine spatial resolution images of the nightside polar ionosphere from 60° to 90° in MLAT. The midnight meridian is represented by a horizontal line through the center of each panel. Shown on the top of each panel is the center time of each exposure. In addition to the 36-s exposure LBHL images (marked as L36s on the right

bottom of each panel), which are used in the identifications of the quiet intervals, the 18-s exposure LBHL images (L18s) are included. L18s images are somewhat noisy, because of the shorter exposure periods. The time separation is 27 s from a L18s image to a L36s image and is 157s from a L36s image to a L18s image.

[21] The images show no brightening at any time, even at the times of earthward flow (1348:13 and 1348:40 UT) shown by red letters. The Geotail location at 1350 UT mapped to 69 MLAT and 23.2 MLT using a corrected Tsyganenko 89 model with $K_p = 0$ [Tsyganenko, 1989]. It
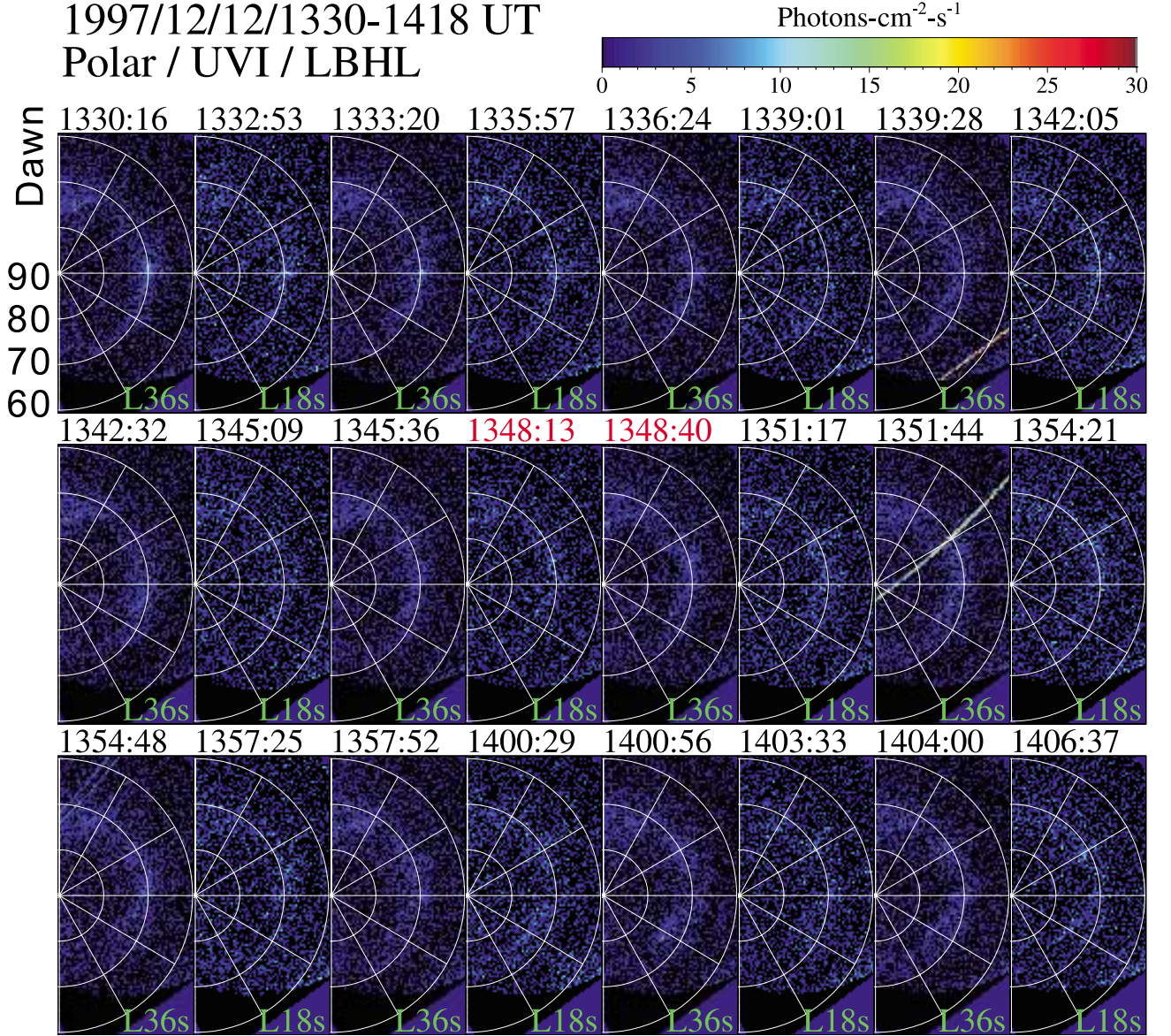
1997/12/12/1330-1418 UT
Polar / UVI / LBHL

Figure 3. The Polar spacecraft ultraviolet images of auroras for the quiet interval when an earthward flow was observed. Shown is a 40-min series of images of the nightside polar ionosphere from 60° to 90° in MLAT with the midnight meridian represented by a horizontal line through the center of each panel. In addition to the 36-s exposure LBHL images (marked as L36s on the right bottom of each panel), which are used in the automatic identifications of the quiet intervals, the 18-s exposure LBHL images (L18s) are shown. The times (1348:13 and 1348:40 UT) of the earthward flow are shown by red letters.

might appear that auroras are slightly brighter around 70° MLAT and 0.5 MLT in the 1354:48 UT panel than in other panels; however, we think this variation in auroras is too weak to be classified as a brightening.

[22] Figure 4 shows an earthward flow event beginning at 1346 UT. Top four panels show the 3-s magnetic field and the next five panels show the 12-s plasma parameters, where V_x (bold line) and $V_{perp,x}$ (thin line) are shown in a single panel. Second panel from the bottom shows the static total pressure and the plasma pressure, where the temperature ratio of ions to electrons was assumed to be five. The bottom panel shows the plasma beta, which is the ratio of the plasma pressure to the magnetic pressure.

[23] The earthward flow was observed at 1346–1353 UT. The plasma beta was higher than unity, suggesting that Geotail was deep in the plasma sheet. Variations in the static total pressure along with a large peak in B_y indicate that the earthward flow was transient. The earthward flow started around 1346 UT and had a peak in the $V_{perp,x}$ (= 126 km s^{-1}) at 1347:42 UT and a peak in the V_x (= 390 km s^{-1}) at 1350:32 UT.

[24] Figure 5a shows energy-time spectrograms of electrons and ions in satellite coordinates, which are close to the GSE coordinates, for the same interval as Figure 4. The top two panels show the counts of electrons from 60 eV q^{-1} to 38 keV q^{-1} streaming earthward and tailward. The bottom
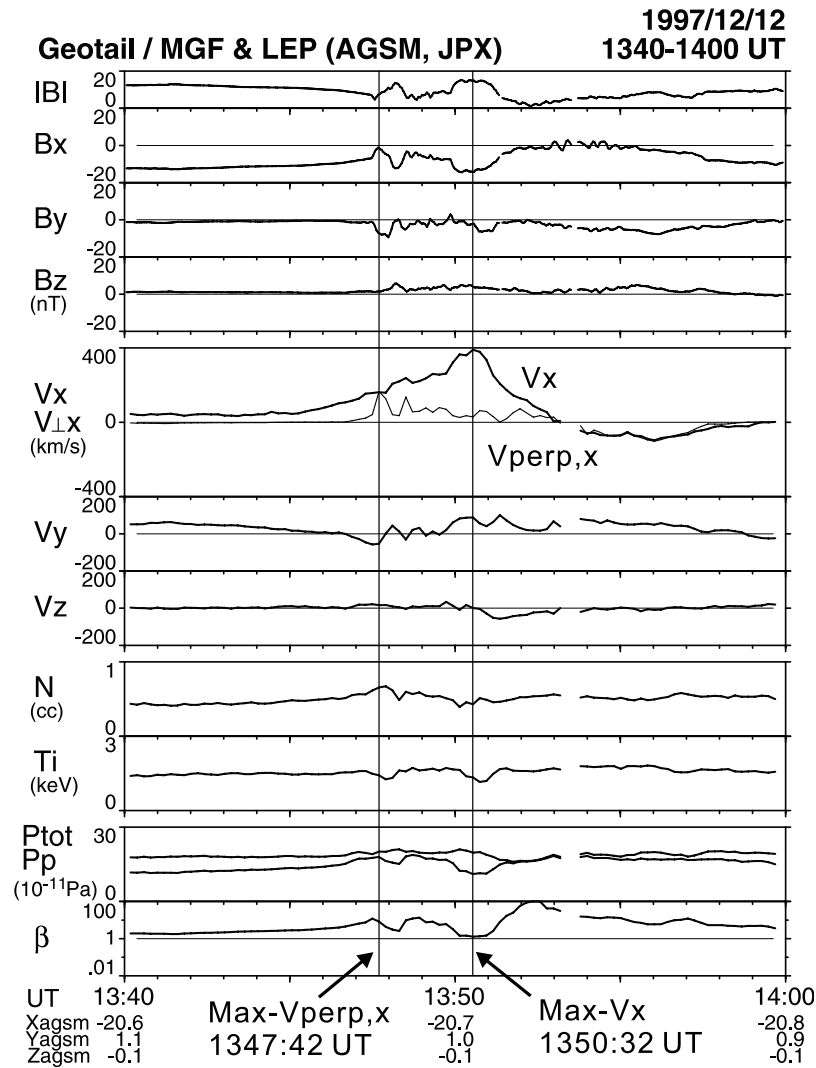
Figure 4. An earthward flow event beginning at 1346 UT, whose auroral conditions were shown in Figure 3. The top four panels show the 3-s magnetic field, and the next five panels show the 12-s plasma parameters. Second panel from bottom shows the static total pressure and the plasma pressure, where the temperature ratio of ions to electrons was assumed to be five. The bottom panel shows the plasma beta, which is the ratio of the plasma pressure to the magnetic pressure.

four panels show ions from 32 eV q^{-1} to 39 keV q^{-1} streaming dawnward, earthward, duskward, and tailward. The counts of the LEP instrument have energy dependences so that higher-energy particles are exaggerated in Figure 5a when compared to the phase space densities. There are enhanced earthward moving ions between 1346 and 1353 UT, while the low-energy part of tailward moving ions gradually disappear from 1348 to 1350 UT. These tendencies are not clear in electron energy-time spectrograms.

[25] Figure 5b shows the slices of the ion velocity distribution functions on the plane including the velocity vector and the magnetic field vector. The plane also contains the $\mathbf{V}_{perp}$ vector and the $\mathbf{V}_{para}$ vector by definition, where $\mathbf{V}_{para} = \mathbf{B}\,(\mathbf{V} \cdot \mathbf{B})/B^2$ and $\mathbf{V}_{perp} = \mathbf{V} - \mathbf{V}_{para}$. The color code indicates the phase space densities (s^3 m^{-6}). At 1347:42 UT when a peak in the $V_{perp,x}$ was observed and the magnetic field was dawnward, ions mostly consisted of a component streaming in the direction (earthward) perpen-

dicular to the magnetic field, except for a dawnward-streaming component. While at 1350:32 when a peak in the V_x was observed and the magnetic field was tailward, the ion velocity distribution shows two components streaming along the magnetic field. The earthward streaming component ($\sim$570 km s^{-1}) is somewhat faster than the velocity moment (390 km s^{-1}), which is shown by a white arrow. This difference is mainly due to the tailward streaming component (-860 km s^{-1}), while the lowest-energy ions ($\sim$100 km s^{-1}) that are slightly lower than the 1-count level do not contribute much. These counterstreaming ions consisting of the earthward streaming denser component and the tailward streaming more energetic component are known as a plasma sheet boundary layer (PSBL) feature [*Forbes et al.*, 1981; *Eastman et al.*, 1984, 1985]. The tailward streaming component is thought to be caused by the near-Earth mirroring of the earthward streaming component [e.g., *Onsager et al.*, 1991]. This mirroring may be
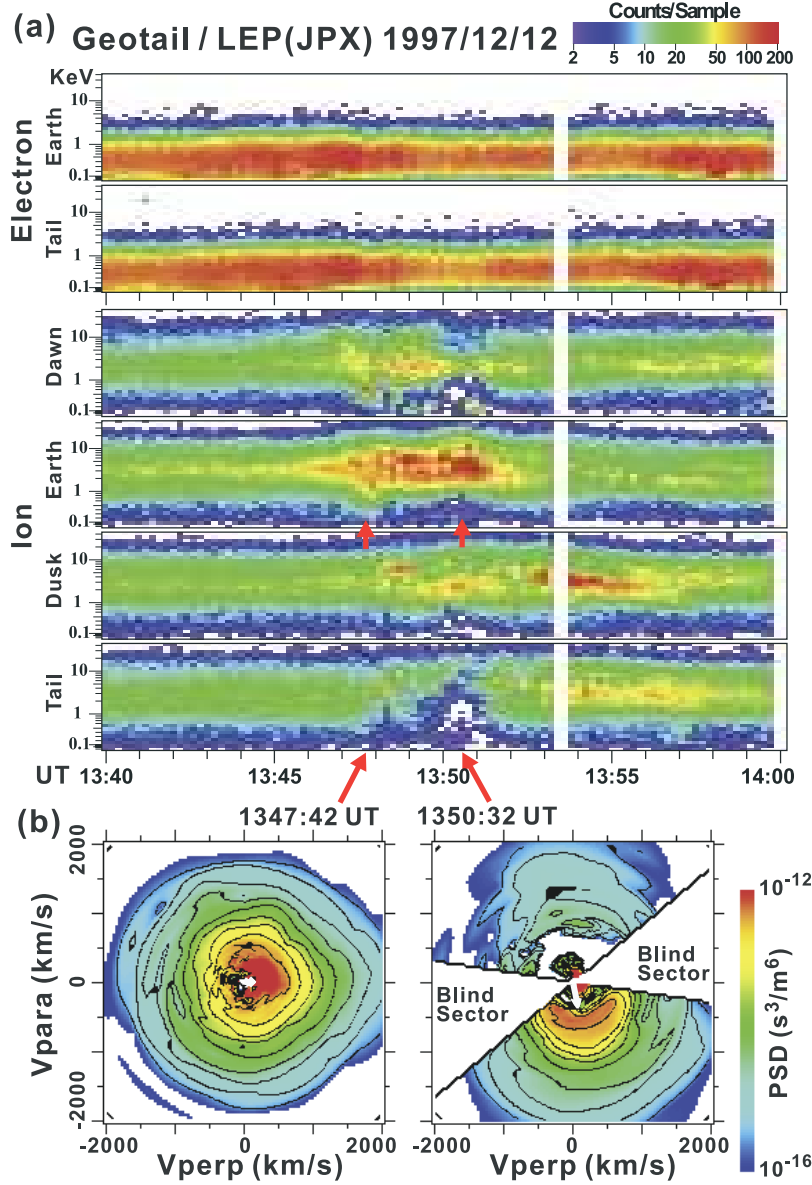
Figure 5. (a) Energy-time spectrograms of electrons and ions for the same interval in Figure 4, shown in satellite coordinates, which is close to the GSE coordinates. The top two panels show electrons from 60 eV q^{-1} to 38 keV q^{-1} moving earthward and tailward. The bottom four panels show ions from 32 eV q^{-1} to 39 keV q^{-1} moving dawnward, earthward, duskward, and tailward. (b) The slices of the ion distribution functions at 1347:42 and 1350:32 UT on the plane including the velocity vector and the magnetic field vector. The plane also contains the V_{perp} vector and the V_{para} vector by definition. White arrows are velocity vectors (velocity moments).

consistent with the fact that the particular flow was not geoeffective. Electron velocity distribution functions (not shown) show a single Maxwellian distribution at 1347:42 UT and field-aligned counterstreaming components at 1350:32 UT.

[26] Figure 6 shows the solar wind parameters measured by the IMP 8 satellite at GSM $(X, Y, Z) = (31, 1, 6)$ R_E. The horizontal bar between 1346 and 1353 UT shows the periods of the earthward flow. The IMF has been northward for more than 1 hour including this interval, and this is consistent with the quiet auroras. There are some small-scale structures in the IMF like around 1334 UT, but their

associations with the tail and with the ionosphere are not clear.

[27] Figure 7 is 1-min ground magnetic field data measured by the 210-meridian magnetometers [*Yumoto and the 210° MM Magnetic Observation Group*, 1996] in the Northern Hemisphere shown by their MLAT from top to bottom. Around 1350 UT when the earthward flow was observed, the Kotel'nyy (KTN) station at 22.5 MLT and 70 MLAT showed a very weak gradual variation of 10 nT in the H component. We think this variation might be associated with the earthward flow, but it is difficult to be sure. The magnetic field variations were smaller than a few nT at
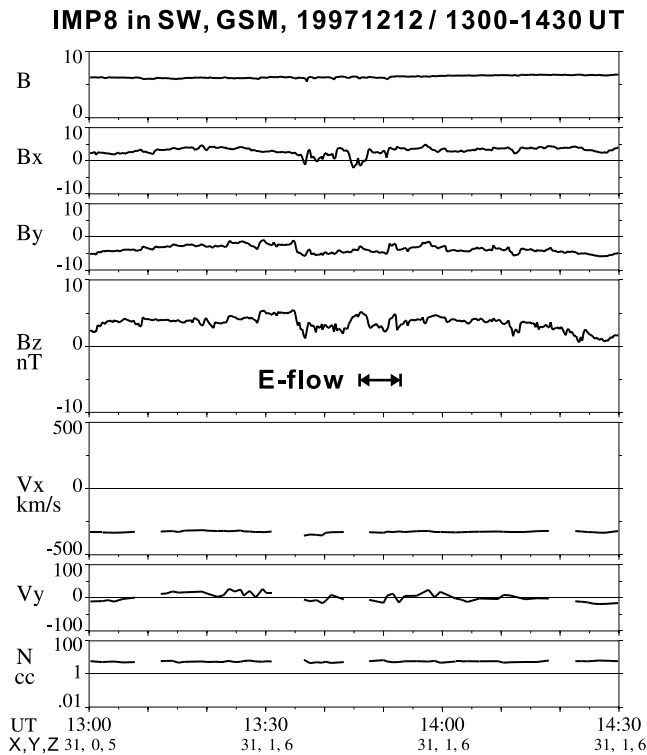
IMP8 in SW, GSM, 19971212 / 1300-1430 UT

Figure 6. The solar wind parameters measured by the IMP 8 satellite at GSM (X, Y, Z) = (31, 1, 6) R_E for the earthward flow event in the tail in Figure 4. The horizontal bar between 1346 and 1353 UT shows the periods of the earthward flow. IMF-Bz has been northward for this interval.

Tixie (TIK, 22.2 MLT, 66 MLAT) and at Zyryanka (ZYK, 23.5 MLT, 60 MLAT). There was no positive bay larger than a few nT in other stations with lower magnetic latitudes. No Pi2 pulsations were inferred from the Kakioka station (23.2 MLT, 30 MLAT) 1-s magnetic field data, and its variation was less than 0.2 nT (not shown). The *Kp* index from 12 to 15 UT was 0. In summary of the ground magnetic field observations, there was no significant disturbance, which is in good agreement with the absence of auroral brightenings in the global images.

5. Discussion and Summary

[28] In this work we first automatically identified quiet intervals with global images and then searched for fast flows (>300 km s^{-1}) in the plasma sheet. As a result, a limited number of earthward parallel fast flows were found but no perpendicular fast flows nor tailward fast flows were found. This result is consistent with the previous findings [*Fairfield et al.*, 1999; *Ieda et al.*, 2001; *Nakamura et al.*, 2001] that clear fast flows were almost always associated with auroral brightenings. The absence of perpendicular fast flows during quiet intervals is suggested by this study, although is not generally conclusive because of the short amount of the quiet intervals (39 hours). Perpendicular fast flows, however, would be at most quite rare with much bigger data set than the 16 months surveyed in this study.

[29] In contrast to the lack of perpendicular fast flows and tailward fast flows, occasional earthward parallel fast flows

were found beyond ∼20 R_E down the tail during quiet intervals. Thus earthward parallel fast flows are not necessarily geoeffective. We would like to emphasize that parallel flows can be transient. A possible explanation of the counterstreaming ions in the PSBL is that the earthward moving component directly comes from the distant neutral line and that the tailward moving component originally comes from the distant neutral line, moves earthward, and then is mirrored near the Earth such that it moves tailward to be observed by a satellite [*Onsager et al.*, 1991]. Since the counterstreaming ions often have the earthward streaming component denser than the tailward streaming component [*Nakamura et al.*, 1992], the resulting velocity moments tend to yield earthward flows. This tendency might lead to a conclusion that there are always earthward fast flows in the PSBL, if the PSBL was identified by the counterstreaming ions. It is known that the counterstreaming ion velocity distribution functions can be found in all geomagnetic activity levels [e.g., *Eastman et al.*, 1984]. This does not mean, however, that there are always fast flows in the outer region of the plasma sheet. If we define the PSBL with the magnetic field and the plasma parameters, not with the counterstreaming ions, the velocity is slow in most cases and fast flows tend to be observed in geomagnetically active intervals [*Baumjohann et al.*, 1988]. The particular earthward flow at 21 R_E in this study was actually transient, since it had variations in the static total pressure and in the magnetic field.

[30] In summary, (1) no perpendicular fast (>300 km s^{-1}) flows were found during quiet intervals. This supports the previous finding that clear fast flows were almost always
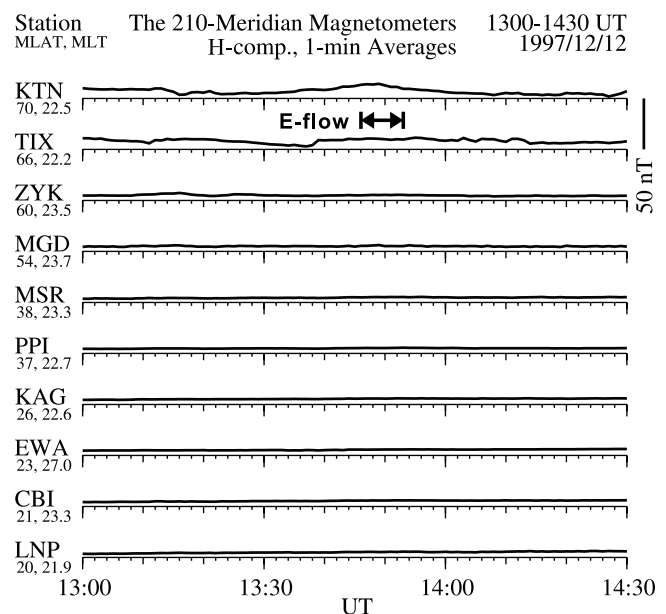

Figure 7. The 210 meridian magnetometer observations of the ground magnetic field in the Northern Hemisphere for the earthward flow event in Figure 4. The horizontal bar between 1346 and 1353 UT shows the periods of the earthward flow. Stations with their magnetic latitudes from the highest to the lowest are shown from top to bottom. There is no significant disturbance on the ground around 1350 UT when the earthward flow was observed.

associated by auroral brightenings. (2) Both earthward parallel fast flows and perpendicular flows faster than 100 km s^{-1} but slower than $\sim$300 km s^{-1} are possible beyond $\sim$20 R_E down the tail even during quiet intervals. The results (1) and (2) suggest that $|V_{\mathrm{perp,x}}|$ $\sim$300 km s^{-1} appears to be a good criterion to statistically separate the geoeffectiveness of flows beyond $\sim$20 R_E. The particular transient earthward parallel fast flow shown in a case study was not geoeffective, and this may be consistent with the tailward moving ion component, which is believed to have been mirrored near the Earth.

References

Baker, D. N., T. I. Pulkkinen, V. Angelopoulos, W. Baumjohann, and R. L. McPherron, Neutral line model of substorms: Past results and present view, *J. Geophys. Res.*, *101*, 12,975–13,010, 1996.

Baker, K. B., and S. Wing, A new magnetic coordinate system for conjugate studies at high latitudes, *J. Geophys. Res.*, *94*, 9139–9143, 1989.

Baumjohann, W., G. Paschmann, N. Sckopke, C. A. Cattell, and C. W. Carlson, Average ion moments in the plasma sheet boundary layer, *J. Geophys. Res.*, *93*, 11,507–11,520, 1988.

Baumjohann, W., G. Paschmann, and C. A. Cattell, Average plasma properties in the central plasma sheet, *J. Geophys. Res.*, *94*, 6597–6606, 1989.

Eastman, T. E., L. A. Frank, W. K. Peterson, and W. Lennartsson, The plasma sheet boundary layer, *J. Geophys. Res.*, *89*, 1553–1572, 1984.

Eastman, T. E., L. A. Frank, and C. Y. Huang, The boundary layers as the primary transport regions of the Earth's magnetotail, *J. Geophys. Res.*, *90*, 9541–9560, 1985.

Fairfield, D. H., T. Mukai, Y. Yamamoto, M. Brittnacher, G. K. Parks, G. D. Reeves, S. Kokubun, D. A. Gurnett, K. Hashimoto, and H. Matsumoto, Earthward flow bursts in the inner magnetotail and their relation to auroral brightenings, AKR intensifications, geosynchronous particle injections and magnetic activity, *J. Geophys. Res.*, *104*, 355–370, 1999.

Forbes, T. G., E. W. Hones Jr., S. J. Bame, J. R. Asbridge, G. Paschmann, N. Sckopkte, and C. T. Russell, Evidence for the tailward retreat of a magnetic neutral line in the magnetotail during substorm recovery, *Geophys. Res. Lett.*, *8*, 261–263, 1981.

Hayakawa, H., A. Nishida, E. W. Hones Jr., and S. J. Bame, Statistical characteristics of plasma flow in the magnetotail, *J. Geophys. Res.*, *87*, 277–283, 1982.

Ieda, A., D. H. Fairfield, T. Mukai, Y. Saito, S. Kokubun, K. Liou, C.-I. Meng, G. K. Parks, and M. J. Brittnacher, Plasmoid ejection and auroral brightenings, *J. Geophys. Res.*, *106*, 3845–3857, 2001.

Kokubun, S., T. Yamamoto, M. H. Acuña, K. Hayashi, K. Shiokawa, and H. Kawano, The Geotail magnetic field experiment, *J. Geomagn. Geoelectr.*, *46*, 7–21, 1994.

Mukai, T., S. Machida, Y. Saito, M. Hirahara, T. Terasawa, N. Kaya, T. Obara, M. Ejiri, and A. Nishida, The Low Energy Particle (LEP) experiment onboard the Geotail satellite, *J. Geomagn. Geoelectr.*, *46*, 669–692, 1994.

Nagai, T., M. Fujimoto, Y. Saito, S. Machida, T. Terasawa, R. Nakamura, T. Yamamoto, T. Mukai, A. Nishida, and S. Kokubun, Structure and dynamics of magnetic reconnection for substorm onsets with Geotail observations, *J. Geophys. Res.*, *103*, 4419–4440, 1998.

Nakamura, M., G. Paschmann, W. Baumjohann, and N. Sckopke, Ion distributions and flows in and near the plasma sheet boundary layer, *J. Geophys. Res.*, *97*, 1449–1460, 1992.

Nakamura, R., W. Baumjohann, M. Brittnacher, V. A. Sergeev, M. Kubyshkina, T. Mukai, and K. Liou, Flow bursts and auroral activations: Onset timing and foot point location, *J. Geophys. Res.*, *106*, 10,777–10,789, 2001.

Nishida, A., H. Hayakawa, and E. W. Hones Jr., Observed signatures of reconnection in the magnetotail, *J. Geophys. Res.*, *86*, 1422–1436, 1981.

Ohtani, S., R. Yamaguchi, M. Nosé, H. Kawano, M. Engebretson, and K. Yumoto, Quiet time magnetotail dynamics and their implications for the substorm trigger, *J. Geophys. Res.*, *107*(A2), 1030, 10.1029/2001JA000116, 2002.

Onsager, T. G., M. F. Thomsen, R. C. Elphic, and J. T. Gosling, Model of electron and ion distributions in the plasma sheet boundary layer, *J. Geophys. Res.*, *96*, 20,999–21,011, 1991.

Paterson, W. R., L. A. Frank, S. Kokubun, and T. Yamamoto, Geotail survey of ion flow in the plasma sheet: Observations between 10 and 50 R_E, *J. Geophys. Res.*, *103*, 11,811–11,825, 1998.

Sergeev, V. A., A. G. Yahnin, R. A. Rakhmatulin, S. I. Solovjev, F. S. Mozer, D. J. Williams, and C. T. Russell, Permanent flare activity in the magnetosphere during periods of low magnetic activity in the auroral zone, *Planet. Space Sci.*, *34*, 1169–1188, 1986.

Shue, J.-H., P. T. Newell, K. Liou, and C.-I. Meng, The quantitative relationship between auroral brightness and solar EUV Pedersen conductance, *J. Geophys. Res.*, *106*, 5883–5894, 2001.

Slavin, J. A., E. J. Smith, D. G. Sibeck, D. N. Baker, R. D. Zwickl, and S.-I. Akasofu, An ISEE 3 study of average and substorm conditions in the distant magnetotail, *J. Geophys. Res.*, *90*, 10,875–10,895, 1985.

Torr, M., et al., A far ultraviolet imager for the international solar-terrestrial physics mission, *Space Sci. Rev.*, *71*, 329–383, 1995.

Tsyganenko, N. A., A magnetospheric magnetic field model with a warped tail current sheet, *Planet. Space Sci.*, *37*, 5–20, 1989.

Yumoto, K., and the 210° MM Magnetic Observation Group, The STEP 210° magnetic meridian network project, *J. Geomagn. Geoelectr.*, *48*, 1297–1309, 1996.

————————————
D. H. Fairfield, Laboratory for Extraterrestrial Physics, NASA Goddard Space Flight Center, Greenbelt, MD 20771, USA.

A. Ieda, Solar-Terrestrial Environment Laboratory, Nagoya University, 3-13 Honohara, Toyokawa, Aichi 442-8507, Japan. (ieda@stelab.nagoya-u.ac.jp)

K. Liou, C.-I. Meng, S.-I. Ohtani, and J.-H. Shue, Johns Hopkins University Applied Physics Laboratory, Laurel, MD 20723, USA.

S. Machida, Department of Geophysics, Kyoto University, Kyoto 606-01, Japan.

T. Mukai and Y. Saito, Institute of Space and Astronautical Science, 3-1-1 Yoshinodai, Sagamihara, Kanagawa 229-8510, Japan.

T. Nagai, Earth and Planetary Sciences, Tokyo Institute of Technology, Tokyo 152-8551, Japan.

G. K. Parks, Space Sciences Laboratory, University of California, Berkeley, Berkeley, CA 94720, USA.